Ion-pairs of structurally related polyoxotantalate clusters and divalent metal cations

Jiahui Chen , Yachun Ma , Dongdi Zhang , Yuqing Yang , Mrinal K. Bera , Jiancheng Luo , Ehsan Raee & Tianbo Liu

View supplementary material

Published online: 09 Oct 2020.

Submit your article to this journal

View related articles

View Crossmark data

Taylor & Francis
Taylor & Francis Group

Check for updates

Ion-pairs of structurally related polyoxotantalate clusters and divalent metal cations

Jiahui Chen[a] (iD), Yachun Ma[b], Dongdi Zhang[a,b], Yuqing Yang[a], Mrinal K. Bera[c], Jiancheng Luo[a], Ehsan Raee[a] and Tianbo Liu[a]

[a]Department of Polymer Science, The University of Akron, Akron, OH, USA; [b]Henan Key Laboratory of Polyoxometalate Chemistry, Henan University, Kaifeng, Henan, PR China; [c]NSF's ChemMatCARS, The University of Chicago, Chicago, IL, USA

ABSTRACT

We report cation-binding behaviors of two $\{P_4Ta_6\}$-type polyoxometalate (POM) clusters with *cis-* and *trans-* subunit geometry in aqueous solution. Two types of divalent cations, Sr^{2+} and Pb^{2+}, possess different binding affinities and sites when interacting with $\{P_4Ta_6\}$. Sr^{2+} ions only form solvent-share ion-pairs with $\{P_4Ta_6\}$, whereas Pb^{2+} ions form contact-ion pairs, selectively interacting with the phosphate groups at different locations and subsequently induce the aggregation of $\{P_4Ta_6\}$, confirmed by isothermal titration calorimetry (ITC), NMR, and small-angle X-ray scattering (SAXS) techniques. Despite Sr^{2+} and Pb^{2+} possessing similar ionic sizes and hydration energies, Pb^{2+} ions with stronger coordination capability result in a closer association with the clusters, eventually to selective interaction that depends on the chelating effect, charge density, and the acidity of phosphate groups at specific sites.

cis-{P₄Ta₆}   trans-{P₄Ta₆}

Pb²⁺ - Contact Ion Pair

Sr²⁺ - Solvent-Shared Ion Pair
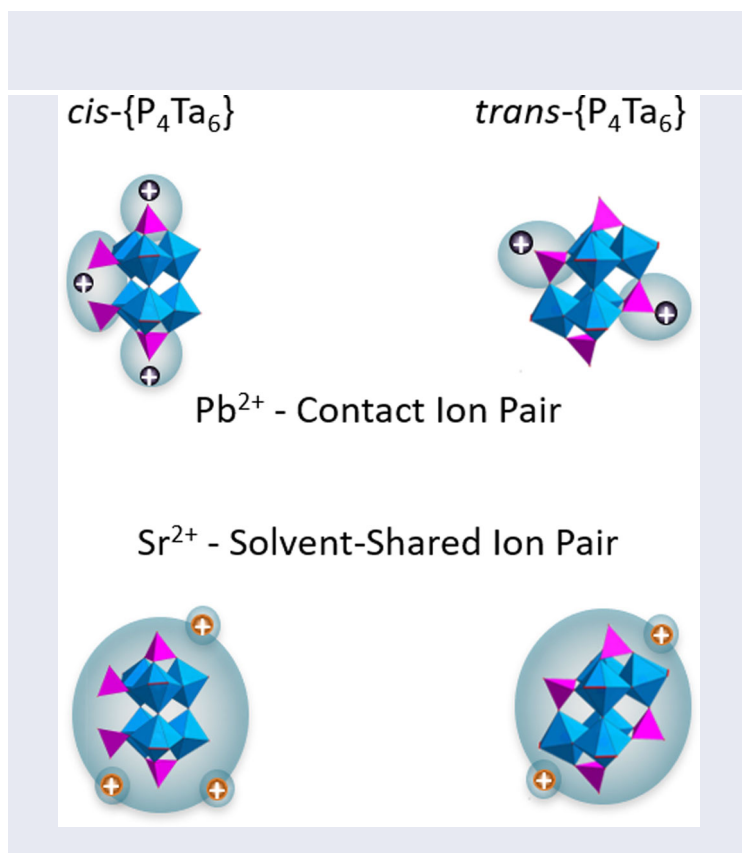
1. Introduction

Polyoxometalates (POMs) are nanosized clusters built from metal oxide octahedra and heteroatoms. POMs have drawn substantial interest due to their applications in electrochemistry, catalysis, magnetism, supramolecular chemistry, *etc*. Among the pioneers in the POM chemistry, Professor En-Bo Wang and his colleagues made important contributions [1–6]. One reason that POMs feature such plentiful properties is due to their structural versatilities. Examples of well-defined structures include Keggin, Dawson, Anderson, Waugh, Strandberg, Lindqvist, Keplerate, Preyssler, *etc*., and some structures exhibit isomerism typically based on rotation of building units [7–9]. Isomers of POMs can be synthesized by carefully tuning the reaction conditions; structure transitions can be achieved in some cases. Slight changes in the isomeric structure can induce significant changes in the properties of POMs. For example, the isomers of Keggin POMs demonstrate different stabilities and redox properties [10]. This leads to an important topic of how to correlate the isomeric structures of a cluster with their properties.

One factor which might play an important role is the interaction between POMs and their counterions in solution [11–16]. Counterion interactions are vital for numerous biochemical processes and functionality of materials [17, 18]. POMs are ideal
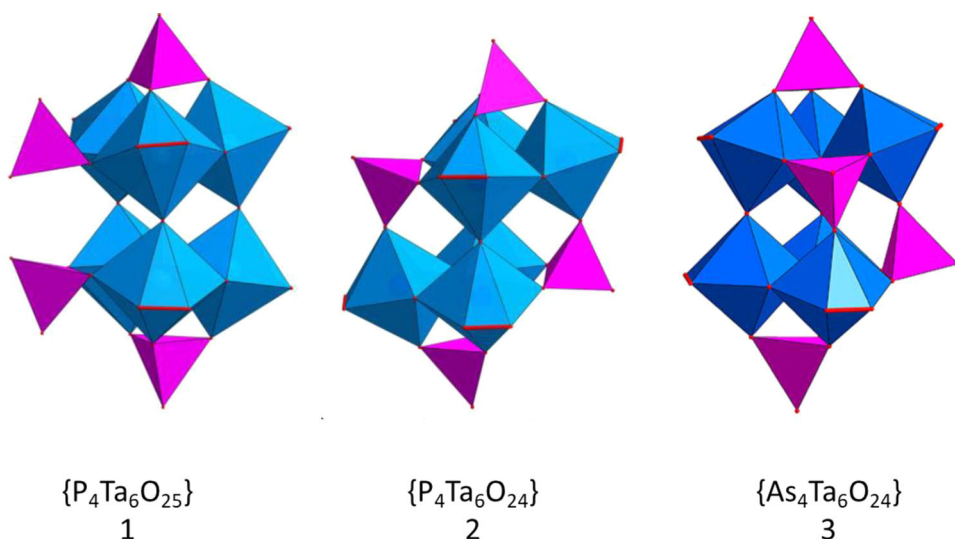
Figure 1. Structure of **1** (left), **2** (middle) and **3** (right). Color code: TaO_7, blue polyhedral; PO_4/ AsO_4, pink polyhedral.

models to study the counterion effects, due to their well-defined, rigid, and yet versatile structures. Counterion effects are also critical for properties of POMs, such as guiding the construction of the POM skeleton during the synthesis. En-Bo Wang *et al.* reported the dimerization of tri-vacant Keggin units by interacting with *trans*-metal counterions. Some counterions can induce isomerization of the tri-vacant units and the dimers containing different counterions demonstrate distinctive electrochemistry properties [19]. Similar observations appeared in other systems [20–22]. Counterions are also important for the solution behavior of POMs. For example, their solubility depends on the counterions [12], and in aqueous solution most POMs show the solubility trend $Li^+ > Na^+ > K^+ > Rb^+ > Cs^+$ for different monovalent counterions. Lighter cations have thicker hydration shells, which prevent them from closely binding with the POMs and result in higher solubility. However, different from extensively studied POMs of group VI (Mo, W), POMs of group V (Nb, Ta) show anomalous solubility trends that exhibit higher solubility with heavier alkali cations [12]. Recent molecular dynamic simulations suggest the formation of contact ion-pairs with some degree of covalent bonding between counterions and the highly charged group V POMs could evoke such anomalous solubility trends [23]. This shows the difference between POMs of group V and group VI, and further study on the group V POM solutions is needed [24].

Recently, we synthesized a series of structurally related Ta-containing POMs (Figure 1): $Cs_3[H_9P_4Ta_6(O_2)_6O_{25}]\cdot 9H_2O$ (**1**), $(CN_3H_6)_6[H_4P_4Ta_6(O_2)_6O_{24}]\cdot 4H_2O$ (**2**) and $Cs_3[Ln(H_2O)_6 \{H_4Ta_6(O_2)_6As_4O_{24}\}]\cdot 7H_2O$ (**3**, Ln = lanthanides) [25, 26]. The phosphorus heteroatoms together with the Ta-oxo framework form $\{P_2Ta_3\}$ half-units, which are *cis* or *trans*-condensed in **1** and **2**, respectively, and in **3** the $\{As_2Ta_3\}$ half-unit rotates to a certain degree. Therefore, the equatorial phosphate ligands are on the same sides in **1** but on the opposite sides in **2**, and in **3** they are in an intermediate situation between **1** and **2**. These compounds represent several examples of polyoxotantalate (POTas) clusters with heteroatoms

Table 1. Thermodynamic parameters of $\{P_4Ta_6\} + nSrCl_2 \rightleftharpoons Sr_n\{P_4Ta_6\} + 2n$ Cl^-, fitted from the ITC experiments of titration $SrCl_2$ salt solution into $\{P_4Ta_6\}$ cluster solutions.

Cluster	1	2
K_a (M^{-1})	7176	3944
ΔH (kJ/mol)	9.06	15.70
ΔS (J/mol·K)	104.2	121.5
n	2	

and have shown potential applications in photoluminescence. However, the properties of these clusters, especially solution behaviors, remain unexplored. There have been numerous studies on the different properties among structurally related group VI POMs. However, due to units with less tendency to nucleate, such structurally related group V POMs are rare and poorly understood. Here we use two structurally similar $\{P_4Ta_6\}$-type clusters (**1** and **2**) as models to study their interaction with two cations, Sr^{2+} and Pb^{2+}, of similar hydration and size, but different coordination capabilities, by using isothermal titration calorimetry (ITC), NMR, and small-angle X-ray scattering (X-ray) techniques.

2. Experimental

2.1. Sample preparation

All chemicals and solvents were purchased from Sigma-Aldrich and used without purification. Two $\{P_4Ta_6\}$-type clusters were synthesized according to the literature [26].

2.2. ^{31}P NMR

^{31}P NMR spectra were measured by a Varian NMR S 500 spectrometer equipped with a 5 mm dual broad band probe in D_2O. All measurements were taken at room temperature. The concentrations of the $\{P_4Ta_6\}$ cluster in solutions were 0.5 mg/mL.

2.3. ITC

The ITC measurements were conducted on a commercial TA Instruments Nano ITC instrument. For a typical experiment, 1.0 mL of 0.5 mg/mL $\{P_4Ta_6\}$ aqueous solution was loaded into the sample cell, and the reference cell was filled with 1.0 mL of deionized water. The 0.25 mL salt solution was titrated into the sample cell each time of 10 μL as volume and 600 seconds between each titration. The background heat was subtracted by titrating the same concentration of the salt solution into water. All thermodynamic parameters were fitted by the independent model.

2.4. SAXS

The small-angle X-ray scattering SAXS experiments were performed at the NSF' ChemMatCARS (15-ID-D) beamline of Advanced Photon Source at Argonne National Laboratory. Data frames were collected at beam energy of 12.0 keV with 1 s exposure
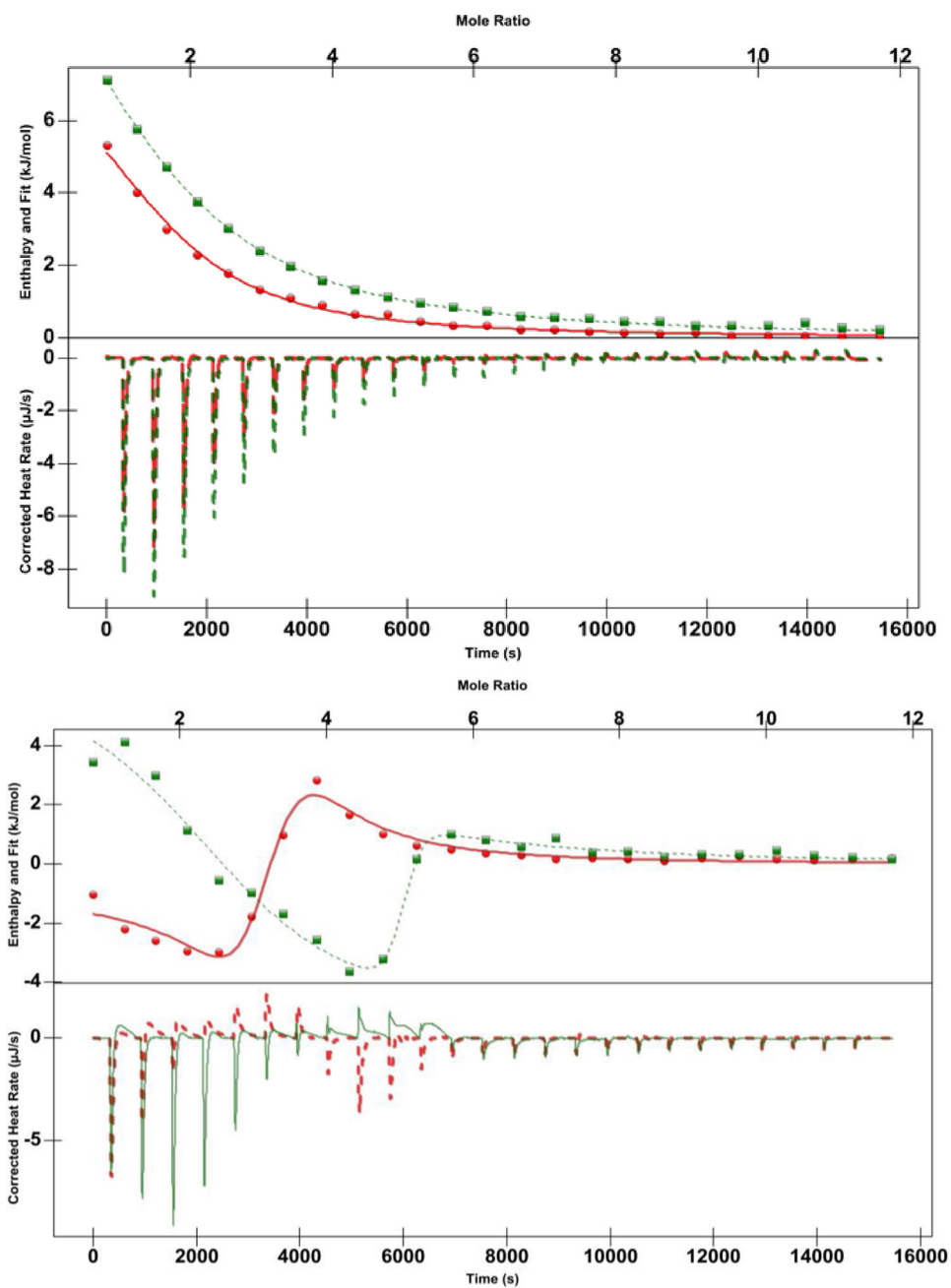
Figure 2. ITC titration curves of 9 mM SrCl$_2$ (top) or Pb(NO$_3$)$_2$ (bottom) into 0.5 mg/mL **1** (red solid lines) or **2** (green dashed lines) solutions, respectively.

time using a Pilatus3 X 300 K detector with 1 mm Si chip and sample to detector distance of 0.57 m. The background was subtracted against water.

Table 2. pH measurements of 0.5 mg/mL {P_4Ta_6} cluster solutions with 12 eq. Sr^{2+} or Pb^{2+} salts. The number in bracket indicates how many protons are released per cluster.

pH	1	2
Without salts	3.6 (1)	5.5 (0)
With 12 eq. $SrCl_2$	2.9 (5)	3.5 (1)
With 12 eq. $Pb(NO_3)_2$	2.7 (9)	3.0 (3)

3. Results and discussion

3.1. Binding affinities of {P_4Ta_6} clusters with Sr^{2+} and Pb^{2+} cations

The binding processes of Sr^{2+} and Pb^{2+} ions with clusters were studied by ITC measurements. ITC experiment measures the heat release upon a titration process, and by fitting the results, the thermodynamic parameters of the binding process, *e.g.*, association constant (K_a), ΔH and ΔS, can be quantitatively measured (Table 1). Details of the binding process can be evaluated from these parameters. Figure 2 shows the ITC results of titration of $SrCl_2$ or $Pb(NO_3)_2$ salt solutions into the cluster solutions. For Sr^{2+} ions, the ITC results demonstrate independent-site binding curves similar for both clusters. The relatively high K_a values, the positive ΔH values and the large entropy gain values suggest an ion-pair formation with hydration shell broken during the cation-cluster interaction [27]. Sr^{2+} shows a slightly higher affinity to **1**, probably because cluster **1** carries more negative charges than cluster **2**, leading to stronger electrostatic interaction. Meanwhile, for Pb^{2+} ions, titrations into solutions of **1** and **2** exhibit two distinct trends of heat release, which cannot be explained by only considering the electrostatic interaction. When titrating Pb^{2+} ions into solution of cluster **1**, the ITC data show two transition points at molar ratios of *ca.* 2 and 4, respectively, while for **2** it only shows a transition point at molar ratio of *ca.* 4. Due to the complex processes, no reliable fitting on the ITC curves can be obtained. SAXS measurements (supporting information Figure S1) confirmed the strong inter-cluster attraction (aggregation) upon adding Pb^{2+} ions into cluster solution, which may correspond to the transition points in the ITC curve at the molar ratio of *ca.* four before saturation. Besides this transition point, the extra transition point at molar ratio of *ca.* two in the Pb^{2+}-cluster **1** titration curve suggests a multi-site binding scenario. However, there is no extra transition point in the titration curve of **2**, suggesting a different binding process compared with **1**.

The deprotonation determines the charges on the clusters and therefore also affects the ion-pair formation. Cluster **1** has nine protons and **2** has four protons as counterions. In aqueous solution, both clusters behave as weak acids and partially release protons. Upon adding salts, some protons can be replaced and released into solution (Table 2). For both clusters, Pb^{2+} can replace most of the protons, while Sr^{2+} can only replace part of the protons.

3.2. Different binding sites of Sr^{2+} and Pb^{2+} cations around {P_4Ta_6} clusters

To confirm the assumption implied from the ITC results and further explore the cation-cluster interaction, ^{31}P NMR experiments were performed to examine the binding location of cations. ^{31}P NMR spectroscopies of **1** or **2** in D_2O solution without extra
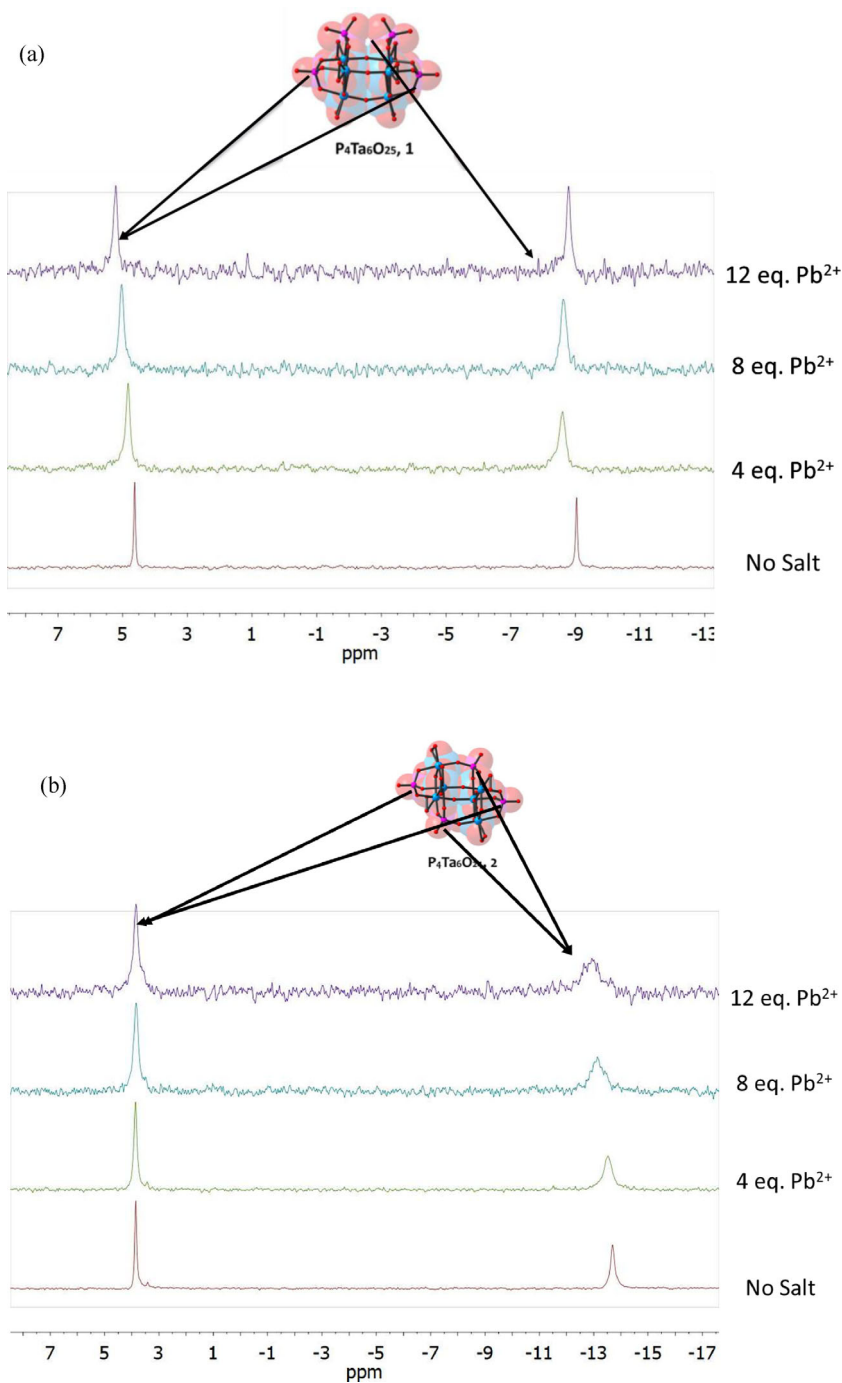
(a)

P4Ta6O25, 1

12 eq. Pb²⁺

8 eq. Pb²⁺

4 eq. Pb²⁺

No Salt

7   5   3   1   -1   -3   -5   -7   -9   -11   -13
ppm

(b)

P4Ta6O₁₂, 2

12 eq. Pb²⁺

8 eq. Pb²⁺

4 eq. Pb²⁺

No Salt

7   5   3   1   -1   -3   -5   -7   -9   -11   -13   -15   -17
ppm

Figure 3. ^{31}P NMR chemical shifts of **1** and **2** with additional metal salts in D_2O. (a) 0.5 mg/mL **1** with $Pb(NO_3)_2$. (b) 0.5 mg/mL **2** with $Pb(NO_3)_2$. (c) 0.5 mg/mL **1** with $SrCl_2$. (d) 0.5 mg/mL **2** with $SrCl_2$.

(c)
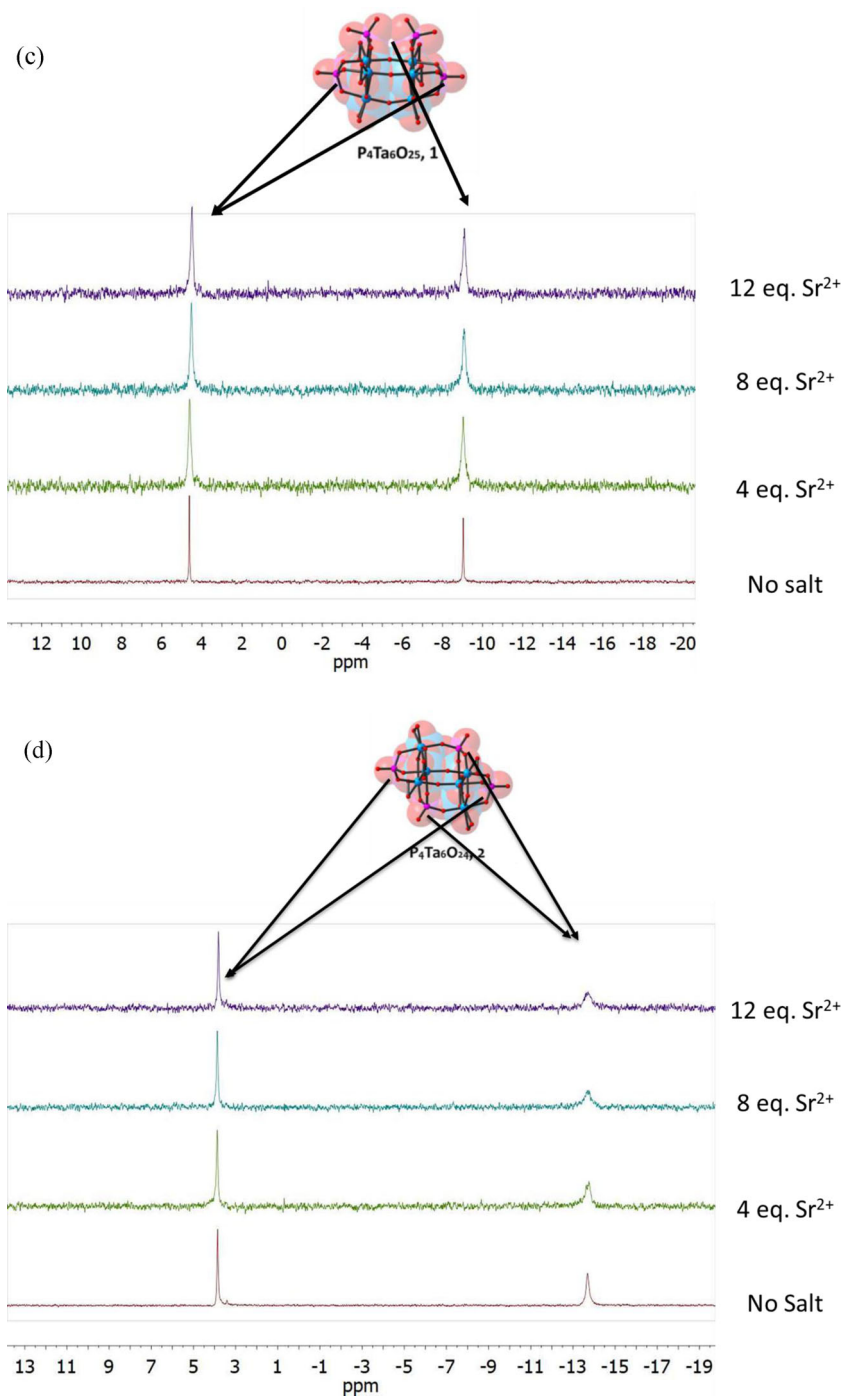

(d)

Figure 3. (Continued)

Table 3. Information of Sr^{2+} and Pb^{2+} ions.

	Ionic radius (Å)	Hydration radius (Å)	Hydration enthalpy (kJ/mol)	Electronegativity (Pauling Scale)
Sr^{2+}	1.28	2.62	−1460	1.0
Pb^{2+}	1.20	2.54	−1460	1.6

Source: References [33–35].

salts exhibit two peaks (Figure 3): the peaks at positive chemical shifts can be assigned to the axial phosphorus atoms, and the peaks at negative chemical shifts can be assigned to the equatorial phosphorus atoms [26]. If added extra cations strongly interact with a specific location on the cluster, a significant change on the chemical shifts of the corresponding phosphorus atom is expected [28]. Therefore, ^{31}P NMR experiment can be used to determine the location of the associated cations.

When Pb^{2+} ions were introduced into solution, ^{31}P NMR results showed that Pb^{2+} ions had different affinities to the phosphate ligands. Figure 3 shows the ^{31}P NMR of 0.5 mg/mL **1** (top) or **2** (bottom) D_2O solution with 0, 4, 8, and 12 eq. $Pb(NO_3)_2$ or $SrCl_2$. The results show that after introducing salts, the peak positions in the ^{31}P NMR spectrum are still close to their original positions, and no new peak appears, suggesting that the structures of the clusters were stable in solution. Upon adding Pb^{2+} ions, some chemical shifts of phosphorus atoms move along the direction of deshielding and show a peak broadening effect. For **1**, the chemical shifts of both types of phosphorus atoms shift, while for **2**, only the chemical shift of the equatorial phosphorus atoms is affected. Therefore, it is concluded that Pb^{2+} ions can form contact ion-pairs with both phosphate ligands in **1**, and in **2** Pb^{2+} ions only form contact ion-pairs with the equatorial phosphate ligands. This is consistent with the ITC results. Upon adding Sr^{2+} ions, the ^{31}P NMR chemical shifts of both clusters are constant, demonstrating a much weaker, indirect Sr^{2+}-cluster interaction than the Pb^{2+}-cluster interaction. Combined with the ITC results which suggest the breakage of hydration shell upon Sr^{2+}-cluster association, a solvent-share type of ion-pair is the best explanation [29].

3.3. Discussion

We previously reported that the type and strength of ion-pair interaction between clusters and cations might vary depending on the charges, hydration energies, and sizes (ionic and hydration radius) of cations [27, 28, 30]. Sr^{2+} and Pb^{2+} are both divalent and share similar size and hydration energy (Table 3). The only difference that can lead to such distinct binding behaviors is their coordination capability. Due to the lanthanide contraction and the relativistic effects, Pb^{2+} can use its 6p orbitals (in some cases 6p orbitals also hybridize with the 6s orbital) to form a complex with ligands, which Sr^{2+} can hardly achieve [31]. Also, Pb(II) has much higher electronegativity than Sr(II). Therefore, when the two cations interact with the clusters, the metal-ligand bonding of Pb^{2+} ion has more covalent character and is stronger than that of Sr^{2+} ion, resulting in contact ion-pairs featuring coordination. The weaker interactions between Sr^{2+} ions and the clusters result in a solvent-shared ion-pair controlled by ionic electrostatic interaction, which usually has insignificant effects on the ^{31}P NMR shifts [32].

Another interesting question is why Pb^{2+} ions bind to different locations on **1** and **2**. For **1**, the higher degree of deprotonation allows it to accommodate more Pb^{2+} ions. Also, the chelating effect of two adjacent equatorial phosphate ligands in the *cis*-conformation facilitates the overall binding strength with Pb^{2+}, which is also observed in the interactions between **3** [25] with cations. Therefore, Pb^{2+} ion is able to interact with both phosphate ligands. On the other hand, **2** carries less charge and may not be able to accommodate Pb^{2+} on all phosphate ligands. Based on the BVS (Bond Valence Sum) calculation, the equatorial phosphorus atoms are at slightly higher oxidation state than that of the axial phosphorus atoms [26]. Therefore, the equatorial phosphate groups are easier to deprotonate and carry negative charges, increasing interaction with Pb^{2+}.

4. Conclusion

We demonstrate distinctive binding behaviors between two similar cations and two structurally related $\{P_4Ta_6\}$-type clusters. Different from the previously reported cation–POM interactions depending on hydration and charge density, two divalent cations, Sr^{2+} and Pb^{2+}, despite similar sizes and hydration energies, show different binding affinities and sites when interacting with the two clusters. Pb^{2+} ions with stronger coordination capability lead to contact ion-pairs with the clusters, while Sr^{2+} ions only form solvent-share ion-pairs. Pb^{2+} ions selectively interact with phosphate groups on different locations and subsequently induce aggregation of the POMs. Due to the difference in acidity and geometry of phosphate ligands and overall cluster charge density, Pb^{2+} ions selectively bind with only equatorial phosphate groups on **2** (*trans*-conformation) and both axial and equatorial phosphate groups on **1** (*cis*-conformation). This work presents the first study on solution behavior of hetero-POTas.

Disclosure statement

No potential conflict of interest was reported by the authors.

Funding

ORCID

Jiahui Chen   http://orcid.org/0000-0002-3861-146X

References

[1] W. Chen. *J. Cluster Sci.*, **31**, 939 (2019). https://doi.org/10.1007/s10876-019-01715-4
[2] L. Chen, W.-L. Chen, X.-L. Wang, Y.-G. Li, Z.-M. Su, E.-B. Wang. *Chem. Soc. Rev.*, **48**, 260 (2019).
[3] X.-B. Han, Z.-M. Zhang, T. Zhang, Y.-G. Li, W. Lin, W. You, Z.-M. Su, E.-B. Wang. *J. Am. Chem. Soc.*, **136**, 5359 (2014).
[4] H. Tan, Y. Li, Z. Zhang, C. Qin, X. Wang, E. Wang, Z. Su. *J. Am. Chem. Soc.*, **129**, 10066 (2007).
[5] Z.-M. Zhang, S. Yao, Y.-G. Li, R. Clérac, Y. Lu, Z.-M. Su, E.-B. Wang. *J. Am. Chem. Soc.*, **131**, 14600 (2009).
[6] P. Yin, Z.-M. Zhang, H. Lv, T. Li, F. Haso, L. Hu, B. Zhang, J. Bacsa, Y. Wei, Y. Gao, Y. Hou, Y.-G. Li, C.L. Hill, E.-B. Wang, T. Liu. *Nat. Commun.*, **6**, 6475 (2015).
[7] R. Thouvenot, M. Fournier, R. Franck, C. Rocchiccioli-Deltcheff. *Inorg. Chem.*, **23**, 598 (1984).
[8] M.T. Pope. In *Heteropoly and Isopoly Oxometalates, Inorganic chemistry concepts*, vol. 8, Springer-Verlag, Berlin, Heidelberg (1983). https://www.springer.com/gp/book/9783662120064.
[9] L.C.W. Baker, J.S. Figgis. *J. Am. Chem. Soc.*, **92**, 3794 (1970).
[10] I.A. Weinstock, J.J. Cowan, E.M.G. Barbuzzi, H. Zeng, C.L. Hill. *J. Am. Chem. Soc.*, **121**, 4608 (1999).
[11] T. Liu. *Langmuir*, **26**, 9202 (2010).
[12] A. Misra, K. Kozma, C. Streb, M. Nyman. *Angew. Chem. Int. Ed. Engl.*, **59**, 596 (2020).
[13] M.T. Pope, A. Müller. *Angew. Chem. Int. Ed. Engl.*, **30**, 34 (1991).
[14] J.M. Poblet, X. López, C. Bo. *Chem. Soc. Rev.*, **32**, 297 (2003).
[15] X. López, J.J. Carbó, C. Bo, J.M. Poblet. *Chem. Soc. Rev.*, **41**, 7537 (2012).
[16] P. Yin, D. Li, T. Liu. *Chem. Soc. Rev.*, **41**, 7368 (2012).
[17] N. Vlachy, B. Jagoda-Cwiklik, R. Vácha, D. Touraud, P. Jungwirth, W. Kunz. *Adv. Colloid Interface Sci.*, **146**, 42 (2009).
[18] C.L. Hill. *J. Mol. Catal. A: Chem.*, **262,** 2 (2007).
[19] C.-Y. Sun, S.-X. Liu, C.-L. Wang, L.-H. Xie, C.-D. Zhang, B. Gao, E.-B. Wang. *J. Coord. Chem.*, **60**, 567 (2007).
[20] P. Yang, Y. Xiang, Z. Lin, B.S. Bassil, J. Cao, L. Fan, Y. Fan, M.-X. Li, P. Jiménez-Lozano, J.J. Carbó, J.M. Poblet, U. Kortz. *Angew. Chem. Int. Ed. Engl.*, **53**, 11974 (2014).
[21] P.C. Burns, M. Nyman. *Dalton Trans.*, **47**, 5916 (2018).
[22] D.-L. Long, H. Abbas, P. Kögerler, L. Cronin. *J. Am. Chem. Soc.*, **126**, 13880 (2004).
[23] M. Segado, M. Nyman, C. Bo. *J. Phys. Chem. B*, **123**, 10505 (2019).
[24] D. Zhang, J. Luo, Y. Ma, T. Zhang, N. Li, C. Li, P. Ma, T. Li, G. Wang, T. Liu, J. Wang, J. Niu. *Inorg. Chem.*, **59**, 6747 (2020).
[25] Z. Liang, H. Wu, V. Singh, Y. Qiao, M. Li, P. Ma, J. Niu, J. Wang. *Inorg. Chem.*, **58**, 13030 (2019).
[26] D. Zhang, Z. Liang, S. Liu, L. Li, P. Ma, S. Zhao, H. Wang, J. Wang, J. Niu. *Inorg. Chem.*, **56**, 5537 (2017).
[27] J. He, H. Li, P. Yang, F. Haso, J. Wu, T. Li, U. Kortz, T. Liu. *Chemistry*, **24**, 3052 (2018).
[28] J. Luo, S. Ye, T. Li, E. Sarnello, H. Li, T. Liu. *J. Phys. Chem. C*, **123**, 14825 (2019).
[29] C. Sgarlata, J.S. Mugridge, M.D. Pluth, V. Zito, G. Arena, K.N. Raymond. *Chemistry*, **23**, 16813 (2017).
[30] J.M. Pigga, J.A. Teprovich, Jr, R.A. Flowers, M.R. Antonio, T. Liu. *Langmuir*, **26**, 9449 (2010).
[31] E.S. Claudio, H.A. Godwin, J.S. Magyar. In *Prog. Inorg. Chem.*, K.D. Karlin (Ed.), Chapter. 1, pp 1–144 (2003).
[32] R. Massart, R. Contant, J.M. Fruchart, J.P. Ciabrini, M. Fournier. *Inorg. Chem.*, **16**, 2916 (1977).
[33] D.W. Smith. *J. Chem. Educ.*, **54**, 540 (1977).
[34] I. Persson. *Pure Appl. Chem.*, **82**, 1901 (2010).
[35] W. Gordy, W.J.O. Thomas. *J. Chem. Phys.*, **24**, 439(1956).